

Interactions among phosphorus, pH and Eh in reforested mangroves, Vietnam: a three-dimensional spatial analysis

Julian F. Oxmann · Luitgard Schwendenmann ·
Rubén J. Lara

Received: 18 July 2008 / Accepted: 3 July 2009 / Published online: 31 July 2009
© The Author(s) 2009. This article is published with open access at Springerlink.com

Abstract Sediment reduction is frequently proposed to increase available phosphorus (P) but several studies found also decreases. Another important factor for P liberation is the pH. We investigated the relative importance of Eh and pH on P cycling in reforested mangroves. Sediment P compounds, pH and Eh were analysed over depth along five transects of two areas in the Saigon River Delta and compared with leaf P levels. A three-dimensional spatial approach was used to investigate pH and Eh effects on P compound distribution at different sediment depth and locate layers of predominant P uptake. Along an inundation gradient, submergence durations of 254 to 2 days per year caused a large Eh gradient within the top 20 cm, whereas Eh response was small within 20–45 cm depth. At individual layers, a correlation between Eh and Al/Fe–P was only found in the upper depth interval (0–20 cm). No significant effect of Eh or Al/Fe–P on Morgan-P (available P) was detected. Minor effects on P composition changes by the Eh were caused through

generally strongly reduced sediment at deeper layers (>20 cm). In contrast, pH variations produced extreme differences in both, Ca–P and available P content at layers of apparently predominant P uptake (>20 cm). As available P was correlated with Ca–P ($p < 0.001$), leaf P ($p < 0.001$) and pH (non linear correlation) it is likely that the pH sensitive Ca–P fraction is a more effective source for mangrove tree growth than Al/Fe–P. The predominant pH effect on P uptake within these reforested mangroves differs from a proposed reduction-governed P cycling in wetlands.

Keywords Calcium phosphate minerals · Inundation · Phosphorus limitation and uptake · Pyrite oxidation · Sediment acidification · Sediment redox potential

Introduction

Mangrove coverage of coastal areas declines world-wide through overexploitation, construction of fish or shrimp ponds and conversions to agricultural use. Exploitations and land reclamations are often uncontrolled or poorly administered in mangrove regions, because management plans are missing (Nam and My 1993). Further, sea level rise might also have an impact on mangroves (Cohen and Lara 2003 and references therein) and hurricane impacts (e.g., Hensel and Proffitt 2002) will probably increase in frequency and intensity due to global climate change. In Vietnam,

J. F. Oxmann (✉) · R. J. Lara
Department of Biogeochemistry, Center for Tropical
Marine Ecology, Fahrenheitstr. 6, 28359 Bremen,
Germany
e-mail: julian.oxmann@zmt-bremen.de;
JOxmann@web.de

L. Schwendenmann
Tropical Silviculture and Forest Ecology, Burckhardt
Institute, University of Göttingen, Büsingenweg 1,
37077 Göttingen, Germany

about 57% of the mangrove area was destroyed during the Second Indochina War. This loss was primarily caused by defoliant spraying in the South (Nam and My 1993), where ca. 105,000 hectares amounting for 36% of the plant cover were destroyed (NAS 1974). Extensive reforestation started after the war and continues to the present day using predominantly seeds and saplings of *Rhizophora apiculata*.

As mangrove reforestation management is of high socio-economical and ecological relevance, it may be more extensively supported by satellite remote sensing (e.g., Hirose et al. 2004) in the future. Reforestation projects should be monitored by biogeochemical and hydrological assessments in order to reduce costs caused by unsuccessful reforestation efforts.

In a previous study (Oxmann et al. 2009) we investigated the nutritional status of reforested mangrove stands in the Saigon River Delta to gain insight in possible limitations to tree growth caused by defoliation-induced changes of geochemical sediment characteristics. We found that the nutritional status is primarily driven by the sediment pH, which in turn had been affected by the Eh. The latter was influenced by inundation and organic matter (OM) decomposition. A lack of OM decomposition by the destruction of the mangrove vegetation can cause sediment oxidation with an accompanying phosphorus (P) deficiency through sediment acidification.

While acid sulphate soils, formed through pyrite oxidation, generally involve a high potential for P deficiency (Dent 1986), sediment pH can also produce drastic effects on P cycling within the relatively narrow pH range 6–7 (Oxmann et al. 2009). A predominantly pH-driven P cycling in these mangrove stands deviates from a major Eh influence on P cycling in regions subjected to frequent or permanent submergence. The latter effect has been subject to a number of studies in both, coastal systems and lakes, because sediment or soil reduction is generally thought to increase available P levels. Nevertheless, transformation processes during reduction and their effects on P solubility are still a matter of debate (Golterman 2001), while the effect of the sediment pH is poorly investigated.

This work investigates pH- and Eh-mediated processes affecting P composition along inundation gradients in order to estimate their relative influence on P uptake. This was attained by a high spatial resolution of physicochemical measurements at a

mangrove site with slightly acidic to alkaline sediment pH along varying topographic elevations and at a nearby acid sulphate site. The latter provided strongly acidic sediment in order to expand the pH range. Systematic relations between pH, Eh, P composition and uptake were analysed using determinations of Morgan-P (available P), Ca-P, Al/Fe-P and leaf P.

Materials and methods

Study area

The study was conducted in the Can Gio Mangrove Biosphere Reserve (CGMBR; 10°22′–10°40′N, 106°46′–107°01′E; UNESCO) of the Saigon River Delta, southern Vietnam (Fig. 1a–e). The CGMBR covers the main part of the Delta (Fig. 1a, dark-grey shade). In the study area, mangrove stands had been exhaustively destroyed by the dispersal of herbicide mixtures during the Second Indochina War. The codenamed Rung Sat Zone within the Saigon River Delta was one of the most heavily sprayed areas in Vietnam. Using a recently developed Geographic Information System that incorporates extensive military data resources of spray missions during the Second Indochina War (Stellman et al. 2003a, b), it was determined (Oxmann et al. 2009) that at least 3,776,560 litres herbicidal agents were sprayed by military aircraft in the Delta. The map presented in Fig. 1a shows the high density of spray paths, especially within the delta, resulting in complete destruction of the mangrove vegetation for military purposes. Some 2,410,825 litres of the defoliant sprayed in the area were likely contaminated with dioxin, dependent on the herbicide mixtures used (Stellman et al. 2003a). In some regions, sediments turned to acid sulphate due to the induced oxidation (Tuan et al. 2002) and remained at these conditions to date. After the war, reforestation began in the CGMBR. At the study sites reforestation took place between 1978 and 1986.

Station selection

Based on a preliminary survey, five transects were established at a strongly acidic site and a control site including 24 sampling stations at 11 sectors

Fig. 1 Study area (adapted from Oxmann et al. 2009).

a Saigon River Delta (shaded dark-grey) and herbicide spray paths (black lines), 1961–1971. **b** Location of the two study sites within the Can Gio Mangrove Biosphere Reserve of the delta. **c** Inundation duration, **d**, **e** location and topographic elevation of the sampling stations at the transects of the control site (**d**) and the strongly acidic site (**e**). Numbers at isolines: elevation in meters above MSL; numbers 1–5: transects; letters A–K: forests sectors (except G: tidal flat). The combination of a transect number with a letter (e.g., 1A) gives the station-ID; CS1/2: directions of cross sections. The map (**a**) was provided using a GIS developed by Stellman et al. (2003a, b)

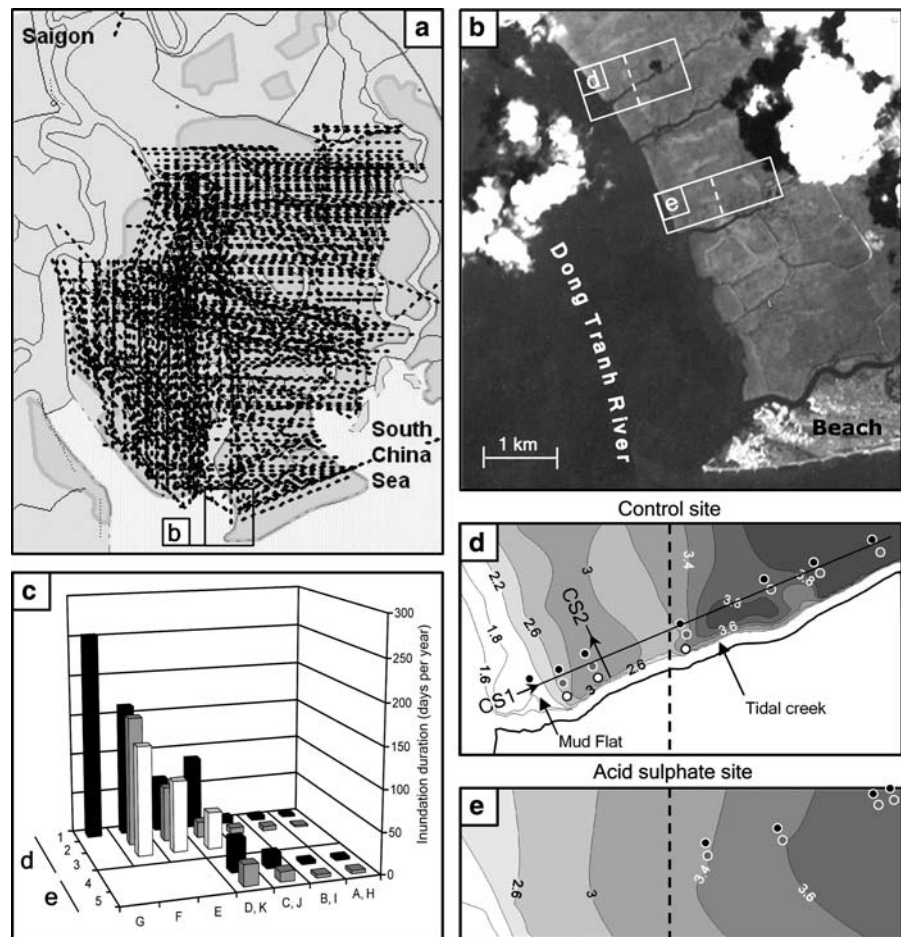


(Fig. 1b–e). The station-ID is given by the combination of the transect number with the letter, which refers to the forest sector (see Fig. 1c). All transects were established perpendicular to the Dong Tranh River. They were selected to investigate the effect of topographic elevation and therefore of inundation on pH, Eh and P distribution patterns in sediment and leaves. The control site (Fig. 1d) and the acid sulphate site (Fig. 1e) were chosen to characterize the effects of acidification on P dynamics and P plant uptake by comparison of sectors with nearly equal inundation frequencies but different sediment pH values. The three transects within the control site were selected to investigate spatial distribution patterns of pH, Eh and P compositions at a mangrove site with slightly acidic to alkaline sediment pH values along varying topographic elevations. Transect 3 was established near a tidal creek to assess its influence on the described parameters, while all other stations were at least 30 m

from tidal creeks. The two transects of the strongly acidic site exhibited lower pH values as a consequence of an earlier shift to acid sulphate conditions.

Topographic elevations, inundation durations (cumulative time of submergence per year) at the stations (Fig. 1c) and relative basal area had been previously determined as described in Oxmann et al. (2009). The unvegetated mud flat station 1G was flooded 254 days/year (Fig. 1c). The vegetated stations were subjected to inundation durations from 163 days/year at the fringe sites to 2 days/year in the hinterland. Concerning the inundation duration a comparable area to the strongly acidic site (H–K) can be defined at the control site (A–G), including only forest sectors A–D (see dashed line in Fig. 1d for separation). As shown in Fig. 2b, all vegetated stations were established in sectors dominated by *Avicennia* (sectors E and F) or *Rhizophora* (all sectors, except E and F). Sectors E and F developed

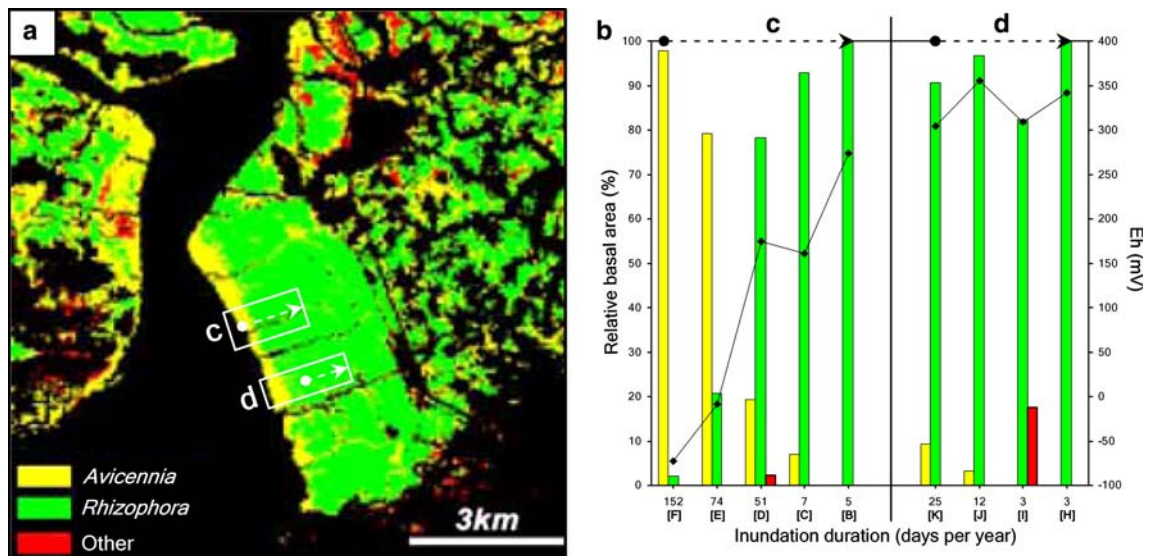


Fig. 2 Mangrove classification image. **a** Mangrove classification within the CGMBR of the Saigon River Delta (adapted with kind permission of K. Hirose). **b** Mangrove forest structure (columns: relative basal area of the genera) and average sediment Eh values (line: 0–20 cm) versus inundation

duration at the control (**c**) and the acid sulphate site (**d**). Capital letters in parenthesis mark different forest sectors. Yellow, green and red colours correspond to genera as shown in key. Dotted arrows mark the transect directions

by natural regeneration, mainly with *Avicennia* species, after failed reforestation with seeds and saplings of *R. apiculata*. The observed occupation of the interface between land and sea by *Avicennia* is in agreement with satellite remote sensing of the delta (Hirose et al. 2004) as shown in Fig. 2a and b.

Sampling and preparation

A piston corer was used to take sediment core samples (one core per station; length: 45 cm; diameter: 9 cm) immediately after inundation had receded. The piston corer had inlets for pH and Eh measurement prior to sectioning. The top of the corer was opened immediately after sampling, while the inlets were opened for measurements at the selected depths and closed afterwards. Sectioned sediments (5 cm slices) were vertically split and the subsamples were kept on ice until sample preparation, which began within a few hours. One subsample was frozen for subsequent particle size analysis. The second subsample, used for nutrient analysis, was prepared by the removal of visible roots, drying at 37°C and grinding with a planetary mill to <300 µm mesh. Phosphorus composition preservation during sample preparation for nutrient analysis is indicated by the following findings:

(1) Heating soils at low temperatures does not significantly affect available P (e.g., Serrasolses et al. 2008). (2) Repeated drying at low temperatures did not significantly change the P composition of sediments (Oxmann et al. 2008). (3) Available P determined after drying reflects in situ available P conditions as shown by significant correlations between leaf P and available P (Boto and Wellington 1983). The analysis of basic sediment properties and its results had been reported in Oxmann et al. (2009).

At each station, one composite leaf sample ($n = 50$ leaves) was collected from the tree closest to the location where the sediment core was taken and another pooled sample ($n = 90$ leaves) from three more trees around this position. The leaves of both samples were divided into subsamples by separating them into three size classes by their width: <2.5 cm (class 1), 2.5–4.0 cm (class 2), >4.0 cm (class 3). Leaves were cleaned with deionised water and tissue paper in order to remove attached salts and other particles. Leaf petioles were removed and the leaves were dried at 60°C, then ground to <80 µm mesh. The powder was kept in a desiccator.

Samples for data presented in this study were taken during the dry season of 2004 and the rainy season of 2005.

Analytical methods and procedures

Physicochemical parameters were measured in the field immediately after separate sampling of each sediment core. Redox potential and pH were determined for each sample in order to develop depth profiles and select characteristic layers for subsequent analyses (see below). Sediment pH was measured with a sulphide resistant, sludge suitable SensoLyt SE (WTW GmbH & Co. KG, Weilheim, Germany) electrode inserted directly into the center of each core section (sections: 9; section interval: 5 cm). The Eh was measured in the same way using two platinum redox micro-probes and an Ag/AgCl reference electrode (Microscale Measurements, The Hague, The Netherlands). The functionality of the redox kit (platinum probes, reference electrode and mV-meter) was tested before each field trip by measuring the potentials of pH 4.0 and 7.0 phosphate buffer solutions saturated with quinhydrone. Measurements of Eh for the Ag/AgCl reference electrode were corrected to the standard hydrogen electrode after calculation of the standard potential at the sediment temperature (Pt-100 insertion temperature sensor) for the reference electrode, which contained 3 M KCl. The endpoint of the redox measurement was monitored by using an A/D-converter and computer to visualize the mV-shift.

Phosphorus analysis of the dried sediment powder included the determination of available P according to a procedure described by Morgan (1941) and a sequential extraction. Available P was determined within each depth interval of sediments taken during the dry season of 2004, whereas depth intervals of 0–5, 10–15, 30–35 cm were selected for available P determination in sediments taken during the rainy season of 2005. Sediment depth intervals of 0–5, 10–15, 30–35 and 35–40 cm were selected for P fractionation. Sequential extraction of Al/Fe–P (by NaOH) and Ca–P (by H₂SO₄) was basically performed as suggested by Kurmies (1972). This method avoids resorption problems through additional Na₂SO₄ extractions and underestimations of NaOH extractable P through initial washing steps with KCl/EtOH solution. The latter eliminate Ca in order to prevent octacalcium phosphate precipitation during the alkaline extraction of Al/Fe–P. Modifications to this procedure were introduced mainly to enhance sample throughput. Detailed descriptions of the modified

fractionation method, the procedure used for the Morgan test and the determination of total leaf P content have been reported in previous publications (Oxmann et al. 2008; Oxmann et al. 2009).

All chemicals were analytical grade. Deionized water was used, purified by a Millipore Milli-Q system (Millipore Corp., MA, USA). All determinations of nutrient levels were duplicated using subsamples.

Data analyses

In order to visualize a trend of the inundation effect on Eh (Fig. 3a) at the different forest sectors, Eh values of each sediment core were averaged over two depth intervals (0–20 cm: $n = 4$ sections; 20–45 cm: $n = 5$ sections) and transects (1/2 and 4/5). Accordingly, inundation durations at the forest sectors were averaged among transects 1/2 and 4/5. Transect 3 has been excluded from averaging, because the tidal creek caused another Eh gradient perpendicular to the inundation effect (see below). For a correlation of Eh versus pH (Fig. 3b), mean values of each sediment core (0–45 cm) comprising nine depth layers were averaged among transects 1/2 and 4/5.

Sediment Eh values of the different layers from sectors A–F were averaged over transects 1 and 2 in order to assess the Eh pattern change with increasing

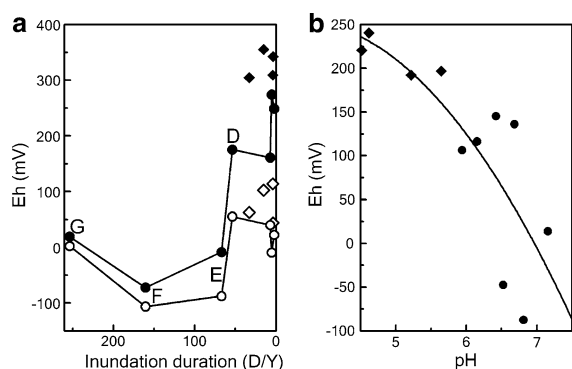


Fig. 3 **a** Redox potential versus inundation duration (days/year). **b** Redox potential versus pH. Data are presented for the control site (circles) and the acidic site (diamonds). Redox potential and pH values were averaged among the different depth intervals and transects (1/2 and 4/5). In **a**: 00–20 cm: ●, ◆; 20–45 cm: ○, ◇. In **b**: 0–45 cm (●, ◆). Capital letters mark sectors with highest inundation-related Eh changes

Table 1 Redox potential versus river distance along the inundation gradient of the control site

| Layer (cm) | Eh (mV) | | | r^c |
|------------|---------------------|-------------------------|------------|-------|
| | Fringe ^a | Hinterland ^a | Δ^b | |
| 0–5 | 42 | 347 | 305 | 0.95 |
| 5–10 | –35 | 338 | 373 | 0.91 |
| 10–15 | –57 | 255 | 312 | 0.79 |
| 15–20 | –60 | 232 | 292 | 0.95 |
| 20–25 | –65 | 76 | 141 | 0.92 |
| 25–30 | –67 | 73 | 140 | 0.70 |
| 30–35 | –72 | 28 | 100 | 0.69 |
| 35–40 | –83 | 29 | 111 | 0.85 |
| 40–45 | –88 | 0 | 88 | 0.48 |

^a Redox values of all forest stations were averaged among transects 1/2. Subsequently, Eh values at fringe and hinterland (ca. 900 m from fringe) were calculated by linear regressions

^b Difference of Eh between fringe and hinterland calculated by linear regressions

^c Correlation coefficients of Eh versus river distance

river distance (Table 1). Using linear regressions of Eh versus river distance (see also r values in Table 1) a depth profile (Fig. 4a) along a cross section perpendicular to the river (CS1 in Fig. 1d) was developed. Linear regression in combination with regular conversion was used in order to generalise the plots in contrast to gridding with raw data by the Kriging method (see below). Sediment Eh values of the different depth layers from transects 1, 2 and 3 were averaged among sectors D, E and F in order to detect the Eh pattern with increasing tidal creek distance. Subsequently, a depth profile (Fig. 4b) along a cross section perpendicular to the tidal creek (CS2 in Fig. 1d) was developed as described above.

Accordingly, average Al/Fe–P values were calculated for an assessment of the Al/Fe–P pattern change with increasing river distance and increasing tidal creek distance. Depth profiles (Fig. 4c, d) along the two cross sections (see Fig. 1d) were obtained as described for the Eh.

Spatial imagery for horizontal plots of Eh, pH, Ca–P and available P distribution was performed using gridding (Kriging method; Davis 1986). Characteristic layers are shown in Fig. 5.

Linear regressions and probability levels given in Fig. 6 and 7 were calculated using raw (not averaged) data.

Results

Interactions among pH, Eh and inundation

At the control site, the average Eh value decreased strongly with increasing inundation duration within the range of 55 (sector D)–65 (sector E) days per year (Fig. 3a). In contrast, the decrease was less pronounced within the range of 65 (sector E)–160 (sector F) days per year (Fig. 3a). Although the unvegetated mud flat station (1G) was flooded for a longer time (254 days per year) than the neighbouring forested stations (sector F), the average Eh values were higher at the mud flat. At the strongly acidic site, average Eh values were comparatively high (Fig. 3a). Across the inundation gradient, Eh variations were less pronounced at the lower depth interval. The standard deviation for all stations was 151 mV at the upper (0–20 cm) and 70 mV at the lower (20–45 cm) depth interval.

Generally, pH values declined with increase in Eh. All sediment pH values were lower at the oxidised, strongly acidic site than at the control site (Fig. 3b).

Seasonal comparability

Three-dimensional spatial pH, Eh and P distribution was comparable between the seasons as indicated by similar mean values among the stations and probabilities of linear correlations between sample values of 2004 and 2005 ($p < 0.01$; data not shown). In the following, data of the rainy season of 2005 will be presented, if not stated differently.

Cross sections of Eh distribution patterns

A significant correlation ($p < 0.001$) of Eh versus river distance was found. According to the linear regressions, the Eh difference within 0–20 cm was relatively large between fringe and hinterland (Table 1). In contrast, this discrepancy was smaller at 20–45 cm. The Eh decreased strongly within the upper layers (<20 cm) at the fringe, while Eh values were only low at deeper layers (>20 cm) in the hinterland. Sediment was strongly reduced at 20–45 cm irrespective of the river distance and, therefore, independent of the inundation duration. The depth profile (Fig. 4a) indicates that, generally, sediments were more reduced across the sediment

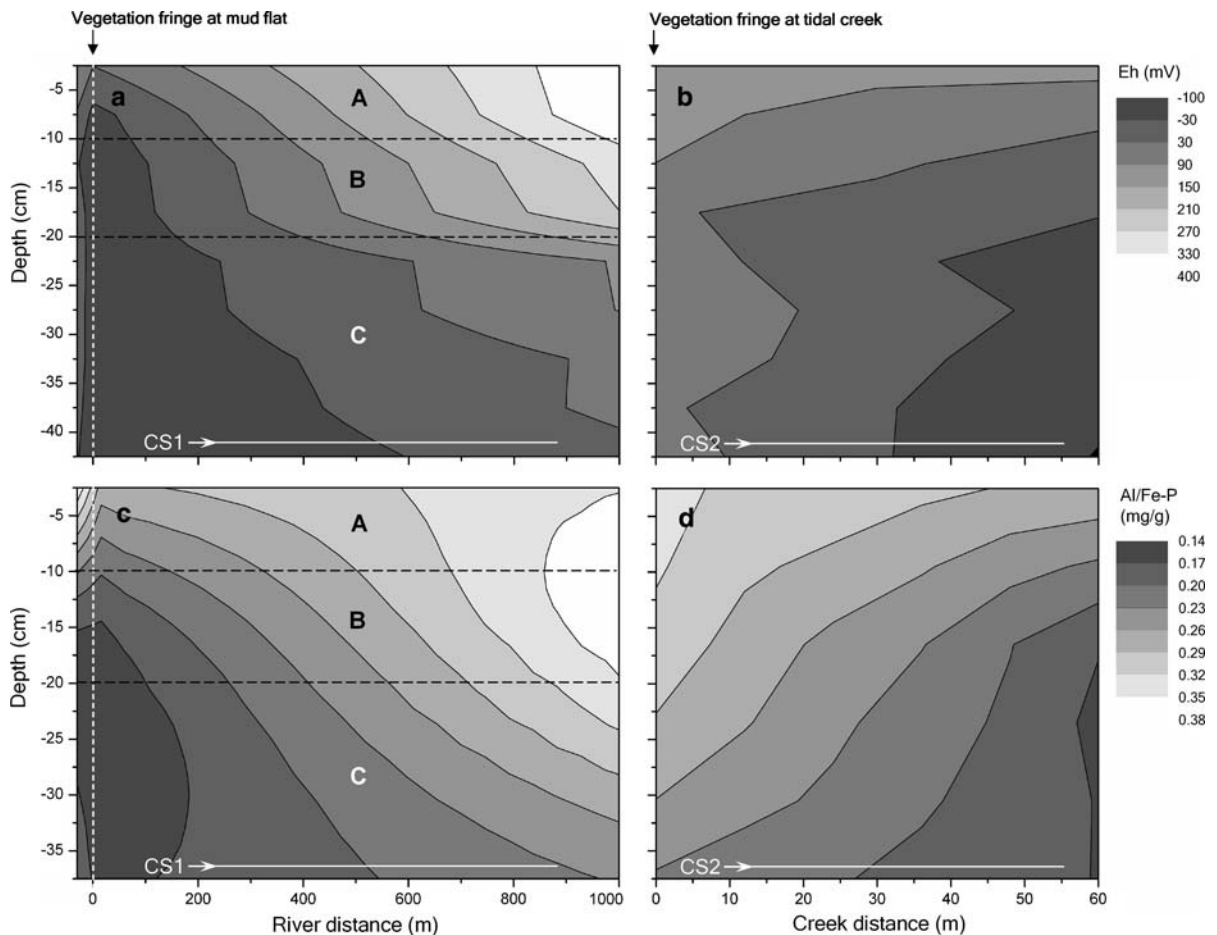


Fig. 4 Distribution patterns of Eh values (**a**, **b**) and Al/Fe–P contents (**c**, **d**) perpendicular to the river (**a**, **c**; CS1) and perpendicular to the tidal creek (**b**, **d**; CS2). The arrows for the cross sections (see Fig. 1) mark increasing distance to the river (CS1) accompanied with decreasing inundation duration and

increasing distance to the tidal creek (CS2). Capital letters in (**a**) and (**b**) mark surface (A), intermediate (B) and deeper sediment layers (C). River and creek distances refer to the vegetation fringes

core with decreasing distance to the vegetation fringe at the mud flat. The difference in the Eh between fringe and hinterland, caused by the different inundation durations, was higher at the surface layers (0–20 cm). Relatively low redox potentials that had been determined at the vegetation fringe within 0–5 cm were measured only below 20 cm in the hinterland. Redox potential values were increased across the sediment core at the unvegetated mud flat.

The aeration by the tidal creek (Fig. 4b) caused increased Eh values across the generally reduced layers within an area of approximately 30 m width near the creek. This Eh increase is comparable to the elevated Eh values at the mud flat (compare with Fig. 4a).

Cross sections of Al/Fe–P distribution patterns

General trends of Al/Fe–P distribution along the cross sections were comparable to the Eh pattern, whilst high Eh values corresponded to high Al/Fe–P levels (Fig. 4c, d).

Significant correlations were found for Eh versus Al/Fe–P (Fig. 6a) at the largest Eh and Al/Fe–P gradients (see Fig. 4a, c) of the control site, at a depth interval of 10–15 cm. These correlations were found at the control site in both, the rainy and the dry season but only at 10–15 cm. No correlations of Eh versus Al/Fe–P were found within depth layers at the strongly acidic site. Nevertheless, Al/Fe–P contents significantly decreased with depth at the control site

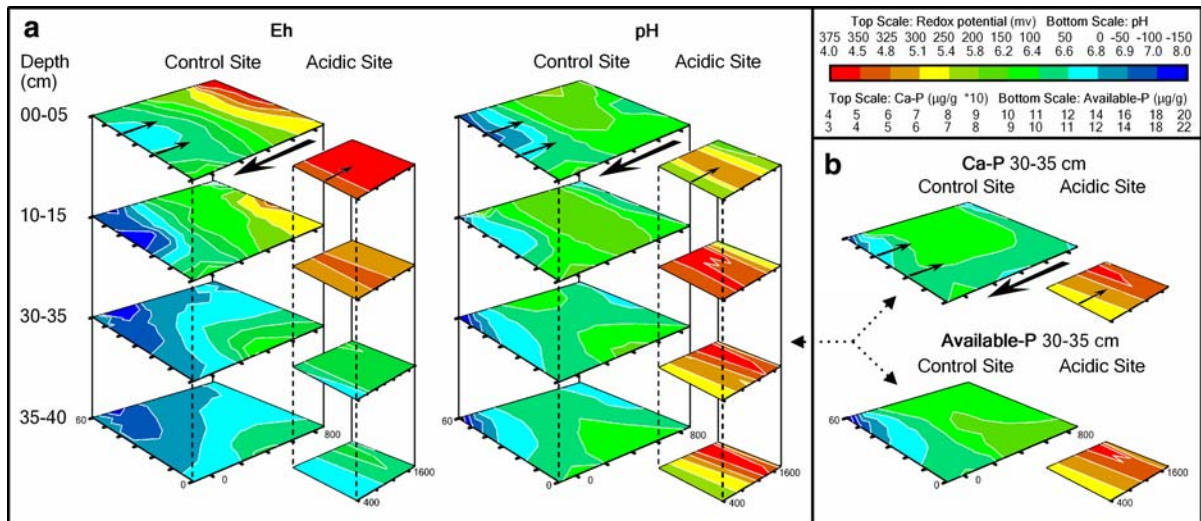


Fig. 5 Three-dimensional spatial patterns of Eh and pH at the control site and the acidic site (**a**). Horizontal Ca-P and available P (Morgan-P) distribution patterns at 30–35 cm depth at the control site and the acidic site (**b**). Colours correspond to values as shown in key. Distances (m) from river or creek vegetation fringes are given at the lowest plots. Small arrows

mark the direction of the rising tide from the river. Large arrows mark the downstream direction of the creek near the control site. Dotted arrows mark comparable plots of pH, Ca-P and available P versus pH: non linear correlations (see Fig. 7)

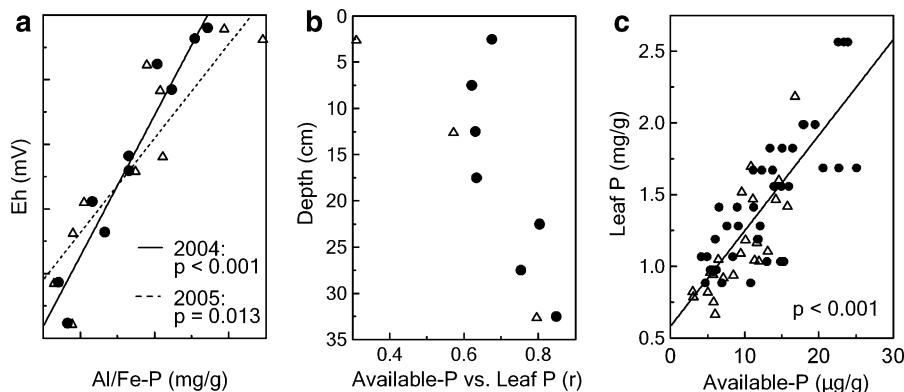


Fig. 6 **a** Redox potential versus Al/Fe-P at 10–15 cm depth. **b** Correlations of leaf P versus available P (Morgan-P) at different sediment layers. **c** Leaf P versus available P for sediments below 20 cm. Samples were taken during the dry

season of 2004 (●) and the rainy season of 2005 (Δ). Data in (**a**) include only values from the control site (no correlation at the acidic site). Significances of correlations are given

(Fig. 4c, d) and the strongly acidic site (Oxmann et al. 2009) mainly by reduction processes.

Three-dimensional distribution patterns

Relatively large Eh differences occurred at the control site in horizontal direction with varying river distance and in vertical direction with increasing sediment depth (Fig. 5a). An Eh decrease is visible with

decreasing river distance, increasing depth and, below 10–15 cm, with increasing tidal creek distance. The acidic site was highly oxidised in the upper sediment layers (< 20 cm). In contrast to the Eh, pH differences between different sediment layers were comparatively small at the control site. At this site, horizontal pH distribution patterns were mainly influenced by alkaline sea water. The acidic site exhibited extremely low pH values below 0–5 cm depth.

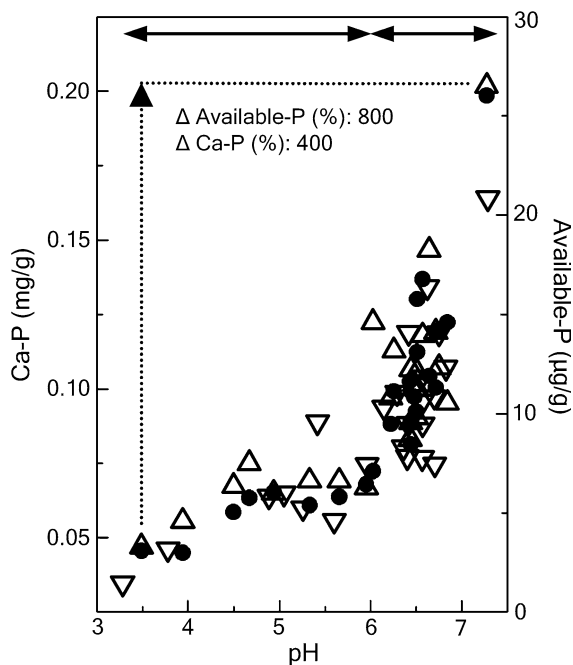


Fig. 7 Ca-P versus pH at 30–35 (Δ) and 35–40 cm (∇) as well as available P (Morgan-P) versus pH at 30–35 cm (\bullet) at the control and the strongly acidic site. Ca-P contents correlated highly significantly ($p < 0.001$) with available P concentrations. *Top arrows* indicate the pH ranges of the strongly acidic (*left arrow*) and the control (*right arrow*) site. An approximate increase of Ca-P (four fold) and available P (eight fold) with pH is given for a pH interval of pH 3.5–7.2 (3.7 increments). Adapted from Oxmann et al. (2009)

At 30–35 cm, a general conformity is visible in the distribution patterns of Ca-P, available P (Fig. 5b) and pH.

P plant uptake

Phosphorus contents in leaves of size class 2 gave the most significant correlations with available P (see Oxmann et al. 2009). Within the top 20 cm, available P did not correlate significantly with leaf P (Fig. 6b). Below a sediment depth of 20 cm, correlations of available P versus leaf P were detected in agreement with increased root biomass at these layers (data not shown). At 30–35 cm, available P correlated significantly with leaf P in both, the rainy and the dry season (Fig. 6b; $p < 0.01$). Pooled data of sediment depths below 20 cm exhibited a highly significant correlation ($p < 0.001$) of available P versus leaf P (Fig. 6c).

A highly significant correlation of available P versus Ca-P ($p < 0.001$) was observed within a depth interval (30–35 cm) of apparently predominant P uptake. Figure 7 indicates that correlations between available P and Ca-P at increased depths were caused by similar variation of these parameters with pH. No correlation between Al/Fe-P and available P was found.

Discussion

This study confirmed that both, sediment pH and Eh have impacts on spatial P distribution patterns in these reforested mangrove stands. However, we found minor effects of reduction processes on differences in P uptake at our study sites. In contrast, sediment pH seemed to be the driving force for P availability across sectors of different forest structures and varying inundation frequencies.

The Eh was found to be dependent on the inundation duration and sediment depth (Figs. 3a, 4) and thus may be related to tree distribution patterns as can be hypothesized from forest structure and Eh data shown in Fig. 2a and b. The initial growth of *Rhizophora* seedlings could be negatively affected by strongly reduced upper sediment layers at the low elevated mangrove fringe. Additionally, the Eh was likely influenced by the aeration of a tidal creek and OM decomposition. The smooth increase of the tidal flat topography suggests that there is a minor difference by aeration between the mud flat station (1G) and the neighbouring station within the forest (1F). Thus, a lower OM decomposition may have caused the elevated redox potentials in the mud flat. Accordingly, sediments of the stations at the strongly acidic site were likely oxidised through the restricted OM decomposition by micro-organisms under acidic conditions. Compared with other soils, the reductive response to flooding of acid sulphate soils is slow due to unfavourable conditions for anaerobic bacteria, such as the extreme acidity, low nutrient status and low content of easily-decomposable OM (Dent 1986). It is suggested that the Eh-induced acidification by the loss of the vegetation is maintained for an extended time, since low pH values may restrict OM decomposition even if the production of OM increases through the subsequently established vegetation. The proposed cycle of high Eh and low pH

values, which promote each other, could be a reason for a prolonged time of sediment acidification. Original conditions may not restore, even if tidal flushing with alkaline seawater and the newly formed vegetation suggest an accelerated re-establishment. Therefore, a complex interaction between Eh and pH is expected. Accordingly, an Eh decrease with increase in pH was observed (Fig. 3b) that could be caused by OM decomposition, pyrite oxidation and tidal effects.

The Al/Fe–P content was significantly correlated with sediment Eh at 10–15 cm (Fig. 6a), while a spatial dependency of both variables is shown by the depth profiles (Fig. 4a–d). A relatively large gradient of sediment Eh, caused by different inundation durations, was found at surface (0–10 cm) and intermediate (10–20 cm) depth intervals. In contrast, the gradient was relatively small at increased depths (> 20 cm). Within depth layers, correlations of Eh versus Al/Fe–P were only detected at an intermediate depth interval (B, Fig. 4a, c), where both parameters exhibited the largest gradients. The lack of a correlation at the surface layer (0–5 cm) was possibly caused by sediment exchange and bioturbation within the upper zone (A, Fig. 4). Moreover, Eh values were not determined directly at the sediment surface, which was likely more oxidised across the transects than determined for the most shallow sediment layer (2.5 cm, see Fig. 4a, b). Patrick and DeLaune (1972) found that the surface remains oxidised and Fe(III) is not reduced within the upper ca. 10 mm during flooding. Phosphorus retention by the oxidised sediment surface could be the reason for the relatively high Al/Fe–P contents (Fig. 4c) across the transects within the surface sediment layer (0–5 cm). Oxidised surface sediments are generally known to retain dissolved P, whereas increased levels of soluble P seem to appear under reducing conditions of deeper sediment layers. This context has been closely referred to adsorption effects. Although these processes are not fully understood, the effects have been related to the reductive dissolution of P binding Fe(III)-oxides in a number of studies (e.g., Hutchison and Hesterberg 2004). For instance, iron seems to occur predominantly in the Fe(III) state in surface sediments and in the Fe(II) state in subsurface sediments of intertidal marsh sediments (Paludan and Morris 1999). However, descriptions of P availability are inconsistent. In contrast to the frequently

proposed increase of available P by reduction due to de-sorption (whereat Mortimer is generally cited, such as Mortimer 1971) several studies found increased P sorption after flooding and decreases in available P caused by submergence (Kuo and Mikkelsen 1979; Sah and Mikkelsen 1986; Sah et al. 1989a, b; Zhang et al. 1993). Increased P sorption is related to amorphous and poorly crystalline oxides and hydroxides of iron (e.g., Krairapanond et al. 1993; Zhang et al. 2003). These controversial results may be partly explained by an initial release of P during the transformations of Fe followed by re-adsorption on amorphous or poorly crystalline Fe-oxides and mixed Fe(II)Fe(III)-hydroxy compounds (e.g., Ponnamperna et al. 1967). A temporal relationship during long-term flooding has been also proposed by Kirk (2004). Provided that there is a temporal relationship, changes along an inundation gradient, involving different submergence durations and frequencies, would be highly difficult to predict. Hence, a spatial pattern of varying, relatively stable steady state conditions along the gradient (see below) would simplify the theoretical considerations.

However, gradients of Eh values at deeper sediment layers (C, Figs. 4a, 5a) were insufficiently large to maintain high differences in the Al/Fe–P content across the inundation zone with increasing depth and, thus, no correlations of Eh versus Al/Fe–P were detected. Therefore, the Eh gradients are likely to have minor impacts on topographically caused differences in P uptake, because correlations of Eh versus Al/Fe–P were only detected at depth layers of apparently reduced P uptake. Correlations of available P versus leaf P were only detected within deeper sediment layers of increased root biomass (Fig. 6b, c). At these layers, sediments were strongly reduced irrespective of the inundation duration. All pe values ($pe = Eh/0.059(V)$ at 25°C) were lower than 1.4 within the depth interval of 20–45 cm and were below the upper pe limit found for soils reduced by submergence during 16 weeks (Kirk 2004). Moreover, no significant effect of Eh or Al/Fe–P on plant available P was observed. As available P correlated highly significantly with leaf P below a sediment depth of 20 cm (Fig. 6c), the Morgan test uses a suitable extraction method for the determination of P available for mangrove P uptake (see also Boto and Wellington 1983).

The potential of a reforestation restriction by acidification is likely higher at elevated areas, where tidal flushing occurs for only a few days per year.

As shown in Fig. 5a, sediment pH values were elevated directly at the river within a relatively small area. This indicates a minor permanent effect of alkaline sea water on sediment pH at elevated areas. Generally, low Eh and high pH values establish by an expanded inundation duration, whereas high Eh and low pH values seem to be relatively stable throughout the extended non flooded periods at higher elevated sites. Accordingly, comparable data for pH, Eh and P forms were acquired within two different years. Further, cores were taken between different tides throughout the seasons, following similar data for the different seasons. Therefore, spatial gradients of these variables seem to be relatively stable over time. Reported changes of physicochemical parameters with time (e.g., Kirk 2004) refer often to single soils or sediments subjected to flooding and do not assess spatial gradients over time. Moreover, these changes were reported for long-term submergence and not for frequent short-term flooding.

Calcium phosphate and pH distribution patterns were comparable at increased depth (Fig. 5). As the Ca–P fraction comprises minerals of different thermodynamic stability, the relatively stable pH distribution pattern (in space and time) likely caused the comparable Ca–P distribution pattern by promoting either precipitation or dissolution of the different minerals. For instance, Laverdiere and Karam (1984) reported the favored formation of less stable calcium phosphate minerals like brushite and OCP in soils with pH > 6. At depth layers of 30–35 and 35–40 cm, which appear to be relevant for P related sediment-plant interactions at the investigated sites, correlations of Ca–P versus pH were found (Fig. 7). As reported in Oxmann et al. (2009), this pH dependency of Ca–P contents was caused by different pH-dependent solubilities of individual Ca–P mineral species. These species were quantitatively determined by a recently developed conversion-extraction method (CONVEX, Oxmann et al. 2008). It has been concluded that the increase in Ca–P content with pH in the range <4 was caused by increased amounts of FAP, while the formation of HAP caused an exponential increase of Ca–P in the pH range 4–7. The precipitation of OCP above pH 7 additionally increased the amount of Ca–P in alkaline sediments.

In contrast to the lack of a correlation between Al/Fe–P and available P, a highly significant correlation ($p < 0.001$) was found for Ca–P versus available P, caused by a similar pH dependency of both, Ca–P and

available P (Fig. 7). This resulted in comparable spatial distribution patterns of Ca–P, available P and pH (Fig. 5a, b). These results suggest that the Morgan test solubilises mainly thermodynamically less stable Ca–P minerals, which seem to fuel P plant uptake. In agreement with this suggestion, Ca–P increased about fourfold with a pH increase from 3.5 to 7.2, whereas available P increased about eightfold within the same pH interval (Fig. 7). Thus, Ca–P is most likely a better available P source for mangrove tree growth than Al/Fe–P, especially if large amounts of thermodynamically less stable Ca–P minerals (e.g., octacalcium phosphate) are present. Consequently, the redox potential could be more relevant for changes in P uptake by its impact on pH (Fig. 3b) than through its direct effects on reduction-induced P liberation, particularly in mangrove areas that exhibit a high acidification potential by pyrite oxidation. However, this assumption is probably not restricted to strongly acidic sediments, because the pH produced extreme changes on Ca–P and available P within the relatively narrow pH range 6–7 (Fig. 7). The predominant control of available P by the sediment pH may be the reason for the lack of a correlation between Eh and available P.

Moreover, no correlation was found for Eh versus available P although carbonate contents within the sediments were very low (see Oxmann et al. 2009). Generally, P-sorption in carbonate systems is less affected by Eh, because relatively more inorganic P is bound to calcium carbonate, than to redox sensitive compounds, or is fixed in minerals like apatite and octacalcium phosphate (Moore and Reddy 1994; Feller et al. 2003). The strongly pH-dependent solubilities of calcium carbonate and calcium phosphates (see also Fig. 7), such as apatite and octacalcium phosphate, imply that the pH is an important factor for P cycling in carbonate systems. Our results have demonstrated that the pH could be also the driving force for P cycling in acidic environments. Further, it is generally known that sediments exhibit a high potential for P deficiency at low pH.

A strong decrease of Al/Fe–P with depth and a comparison of Eh and Al/Fe–P patterns (Fig. 4) suggest that the Eh likely causes effects on P cycling and P uptake in comparison to less reduced environmental settings. However, no spatial change of P plant uptake by inundation-induced Eh variation was detectable. With respect to mangrove reforestation,

the reforestation phase may cause Eh dependent spatial variation in plant growth, if seedlings mainly acquire P from upper sediment layers. These layers likely exhibit large spatial differences in Eh. In such a case, more frequently inundated areas could provide conditions for enhanced P uptake. However, less stable Ca–P species may prevail at topographically lower-laying sites due to increased pH and therefore likely cause a positive effect on P plant uptake. The latter context shows that an innovative experimental setup is needed to discriminate between effects of different parameters that vary in the same geographic direction by a high-order driver, such as the tide. A more detailed insight in P species composition by an adequate method, such as the CONVEX method, may provide a worthwhile contribution for future investigations involving P-dynamics, as shown by the determination of high octacalcium phosphate contents at the mangrove fringe (Oxmann et al. 2009). Finally, P speciation through CONVEX or x-ray adsorption near edge structure spectroscopy may support the investigation of measured P releases from anoxic sediments. There is reason for considering also other factors (see Golterman 2001) than the release by reduction of a $\text{Fe}(\text{OOH})\sim\text{P}$ complex, only. In agreement with the close relations between Ca–P, available P, leaf P and pH found in this study, Golterman (2001) proposed a release of P by the solubilisation of a Ca–P compound (apatite).

Acknowledgments We thank Quynh Huong Pham for assisting us in the field and taking care of sampling permits in Vietnam under the management of the Department of Botany and Ecology, University of Natural Sciences, Ho Chi Minh City. We acknowledge Antje and Beate Bierschenk for their help with lab analyses at the Center for Tropical Marine Ecology. An anonymous reviewer provided valuable comments on an earlier version of this manuscript. This study was carried out as a part of the German-Vietnamese collaboration project “Can Gio” and was funded by the German Research Foundation.

Open Access This article is distributed under the terms of the Creative Commons Attribution Noncommercial License which permits any noncommercial use, distribution, and reproduction in any medium, provided the original author(s) and source are credited.

References

- Boto KG, Wellington JT (1983) Phosphorus and nitrogen nutritional status of a northern Australian mangrove forest. *Mar Ecol Prog Ser* 11:63–69
- Cohen MCL, Lara RJ (2003) Temporal changes of mangrove vegetation boundaries in Amazonia: Application of GIS and remote sensing techniques. *Wetl Ecol Manag* 11: 223–231
- Davis JC (1986) Statistics and data analysis in geology, 2nd edn. Wiley, New York
- Dent D (1986) Acid sulphate soils: a baseline for research and development. ILRI publication 39, Wageningen
- Feller IC, McKee KL, Whigham DF, O'Neill JP (2003) Nitrogen vs. phosphorus limitation across an ecotonal gradient in a mangrove forest. *Biogeochemistry* 62:145–175
- Golterman HL (2001) Phosphate release from anoxic sediments or ‘What did Mortimer really write?’. *Hydrobiologia* 450:99–106
- Hensel P, Proffitt CE (2002) Hurricane Mitch: acute impacts on mangrove forest structure and evaluation of recovery trajectories: executive summary. USGS Open File Report 03-182
- Hirose K, Syoji M, Hang HTM, Anh NH, Triet T, Nam VN (2004) Satellite data application for mangrove management. International Symposium on Geoinformatics for Spatial Infrastructure Development in Earth and Allied Sciences
- Hutchison KJ, Hesterberg D (2004) Dissolution of phosphate in a phosphorus-enriched ultisol as affected by microbial reduction. *J Environ Qual* 33:1793–1802
- Kirk G (2004) The biogeochemistry of submerged soils. Wiley, West Sussex
- Krairapanond A, Jugsujinda A, Patrick WH (1993) Phosphorus sorption characteristics in acid sulfate soils of Thailand - Effect of uncontrolled and controlled soil redox potential (Eh) and pH. *Plant Soil* 157:227–237
- Kuo S, Mikkelsen DS (1979) Distribution of iron and phosphorus in flooded and unflooded soil profiles and their relation to phosphorus adsorption. *Soil Sci* 127:18–25
- Kurmies B (1972) Zur Fraktionierung der Bodenphosphate. *Die Phosphorsäure* 29:118–149
- Laverdiere MR, Karam A (1984) Sorption of phosphorus by some surface soils from Quebec in relation to their properties. *Commun Soil Sci Plant Anal* 15:1215–1230
- Moore PA, Reddy KR (1994) Role of Eh and pH on phosphorus geochemistry in sediments of Lake Okeechobee, Florida. *J Environ Qual* 23:955–964
- Morgan MF (1941) Chemical soil diagnosis by the universal soil testing system. *Connect Agric Exp Station Bull* 450
- Mortimer CH (1971) Chemical exchanges between sediments and water in Great Lakes—Speculations on probable regulatory mechanisms. *Limnol Oceanogr* 16:387–404
- Nam VN, My TV (1993) Mangrove for production and protection, a changing resource system: case study in Can Gio District, Southern Vietnam. The Food and Agriculture Organisation of the United Nations (FAO), Regional Wood Energy Development Programme in Asia, Bangkok. Field Document No. 43
- National Research Council Committee on the Effects of Herbicides in Vietnam (1974) The effects of herbicides in South Vietnam. Part A. Summary and conclusions. National Academy of Sciences Press, Washington
- Oxmann JF, Pham QH, Lara RJ (2008) Quantification of individual phosphorus species in sediment: a sequential

- conversion and extraction method. *Eur J Soil Sci* 59: 1177–1190
- Oxmann JF, Pham QH, Schwendenmann L, Stellman JM, Lara RJ (2009) Mangrove reforestation in Vietnam: the effect of sediment physicochemical properties on nutrient cycling. *Plant Soil* (in press). doi [10.1007/s11104-009-0003-4](https://doi.org/10.1007/s11104-009-0003-4)
- Paludan C, Morris JT (1999) Distribution and speciation of phosphorus along a salinity gradient in intertidal marsh sediments. *Biogeochemistry* 45:197–221
- Patrick WH, DeLaune RD (1972) Characterization of the oxidized and reduced zones in flooded soils. *Soil Sci Soc Am Proc* 36:573–576
- Ponnamperuma FN, Tianco EM, Loy TA (1967) Redox equilibria in flooded soils. I. Iron hydroxide systems. *Soil Sci* 103:374–382
- Sah RN, Mikkelsen DS (1986) Sorption and bioavailability of phosphorus during the drainage period of flooded-drained soils. *Plant Soil* 92:265–278
- Sah RN, Mikkelsen DS, Hafez AA (1989a) Phosphorus behavior in flooded-drained Soils. 2. Iron transformation and phosphorus sorption. *Soil Sci Soc Am J* 53:1723–1729
- Sah RN, Mikkelsen DS, Hafez AA (1989b) Phosphorus behavior in flooded-drained soils. 3. Phosphorus desorption and availability. *Soil Sci Soc Am J* 53:1729–1732
- Serrasolses I, Romanyà J, Khanna PK (2008) Effects of heating and autoclaving on sorption and desorption of phosphorus in some forest soils. *Biol Fertil Soils* 44:1063–1072
- Stellman JM, Stellman SD, Christian R, Weber T, Tomasallo C (2003a) The extent and patterns of usage of Agent Orange and other herbicides in Vietnam. *Nature* 422:681–687
- Stellman JM, Stellman SD, Weber T, Tomasallo C, Stellman AB, Christian R (2003b) A geographic information system for characterizing exposure to Agent Orange and other herbicides in Vietnam. *Environ Health Perspect* 111:321–328
- Tuan LD, Oanh TTK, Thanh CV, Qui ND (2002) The management board for Ho Chi Minh City environmental protection forests. Can Gio Mangrove Biosphere Reserve. Publisher of Agriculture, Hồ Chí Minh City
- Zhang YS, Werner W, Sun X (1993) Phosphorus adsorption and desorption in paddy soils as affected by organic manure and cellulose. *Agric Biol Res* 46:286–294
- Zhang YS, Lin XY, Werner W (2003) The effect of soil flooding on the transformation of Fe oxides and the adsorption/desorption behavior of phosphate. *J Plant Nutr Soil Sci* 166:68–75